國立海洋生物博物館
NATIONAL MUSEUM OF MARINE BIOLOGY & AQUARIUM
Platax 17: 1-26, 2020
doi: 10.29926/platax.202012_17.0002

A coral transcriptome in the Anthropocene as an "alternative stable state"

Anderson B. Mayfield[1,2*] and Chii-Shiarng Chen[3,5]

[1]Cooperative Institute for Marine & Atmospheric Studies, University of Miami, Miami, FL 33149, USA

[2]Atlantic Oceanographic & Meteorological Laboratory, National Oceanic & Atmospheric Administration, Miami, FL 33149, USA

[3]National Museum of Marine Biology & Aquarium, Checheng, Pingtung 944, Taiwan

[4]Graduate Institute of Marine Biotechnology, National Dong-Hwa University, Checheng, Pingtung 944, Taiwan

[5]Department of Marine Biotechnology & Resources, National Sun Yat-Sen University, Kaohsiung 80424, Taiwan

*Corresponding author. Email: anderson.mayfield@noaa.gov or abm64@miami.edu

Abstract

In contrast to many coral reefs across the globe, those of Taiwan's deep south had, until the summer of 2020, not generally been greatly affected by climate change-driven seawater temperature rise. This has been attributed to the effects of cold-water upwelling, which naturally cools reefs within Nanwan Bay during the warmest times of the year; episodic upwelling has also thermally "hardened" the resident corals, and prior works sought to uncover the molecular basis of such thermotolerance in colonies of the model coral *Pocillopora acuta* collected from Nanwan Bay by exposing fragments to sustained high temperatures (30°C) in laboratory mesocosms for nine months. Although all corals ultimately acclimated to this hypothetically stress-inducing temperature *ex situ*, the dinoflagellate endosymbionts residing within the host corals' gastrodermal cells collectively displayed a concerted, sustained mRNA-level response to prolonged high-temperature exposure. Herein we used univariate, multivariate, and modeling approaches with the same transcriptomic dataset and identified numerous genes only expressed by corals at high temperatures; although this finding was not generally supported by real-time PCR, these genes may nevertheless be of use to those seeking to develop biomarker assays or molecularly biology-trained predictive models for identifying corals displaying "alternative stable states," in which their cellular biology has fundamentally changed on account of having acclimatized to chronically high temperatures.

Keywords: Acclimation, Coral reefs, Dinoflagellate, Gene expression, Molecular biology, Taiwan

Introduction

Although global climate change (GCC; Mayfield & Gates, 2007; Hoegh-Guldberg et al., 2017) and other, localized anthropogenic insults like seawater pollution (Huang et al., 2011; Lin et al., 2018; Mayfield et al., 2019b) threaten coral reefs (Gates, 1990; Brown, 1997) and other marine ecosystems (e.g., seagrass beds [Liu et al., 2020] & tidal flats [Chen et al., 2017, 2019]), coral reefs of Southern Taiwan have generally thrived with respect to coral abundance and diversity (Ribas-Deulofeu et al., 2016, but see Liu et al., 2009, 2012 for information on local stressor regimes.). The marked resilience noted in the framework-building scleractinians has been hypothesized to be due to the thermodynamic nature of Nanwan Bay (Mayfield et al., 2012a), which experiences extreme upwelling events in the boreal summer (Lee et al., 1997) that result in large shifts in temperature (6-9°C/day), nutrient levels, and other seawater quality parameters. On a global scale, reef cooling via upwelling has indeed been shown to protect, or even rescue, coral reefs from bleaching, especially when upwelling occurs during summer (Randall et al., 2020; Storlazzi et al., 2020; but see Chollott et al., 2010). More generally, highly variable seawater quality conditions have been shown to stress-harden corals (Mayfield et al., 2011, Safaie et al., 2018). Unfortunately, even the presumed thermal conditioning as a result of habitual upwelling was insufficient to safeguard Nanwan corals against bleaching in the summer of 2020; whether these corals recover and are then even further able to combat future high-temperature episodes (sensu Brown et al., 2000) remains to be determined. If no acclimatization or adaptation occurs, Taiwan's coral reefs are projected to bleach annually by 2023 according to a newly released report from the United Nations Environmental Programme (sp; UNEP, 2020); only ~10% of Taiwan's reefs are anticipated to resist "annual severe bleaching" beyond 2030.

Although highly GCC-tolerant corals exist across the globe (e.g., Krueger et al., 2017; Putnam et al., 2017; Enochs et al., 2020), even corals from seemingly "pristine" locales hundreds of kilometers from human settlements (Fig. 1) display perceivably "stressed" cellular phenotypes (Mayfield et al., 2016a, 2017a-c, 2019a, 2018b-c, in prep; Mayfield, in review). For instance, heat shock proteins, oxidative stress markers, and other genes/proteins involved in the cellular stress response (CSR) are constitutively expressed even during low-temperature periods (Mayfield et al., in review). Instead, proteins involved in other cellular processes,

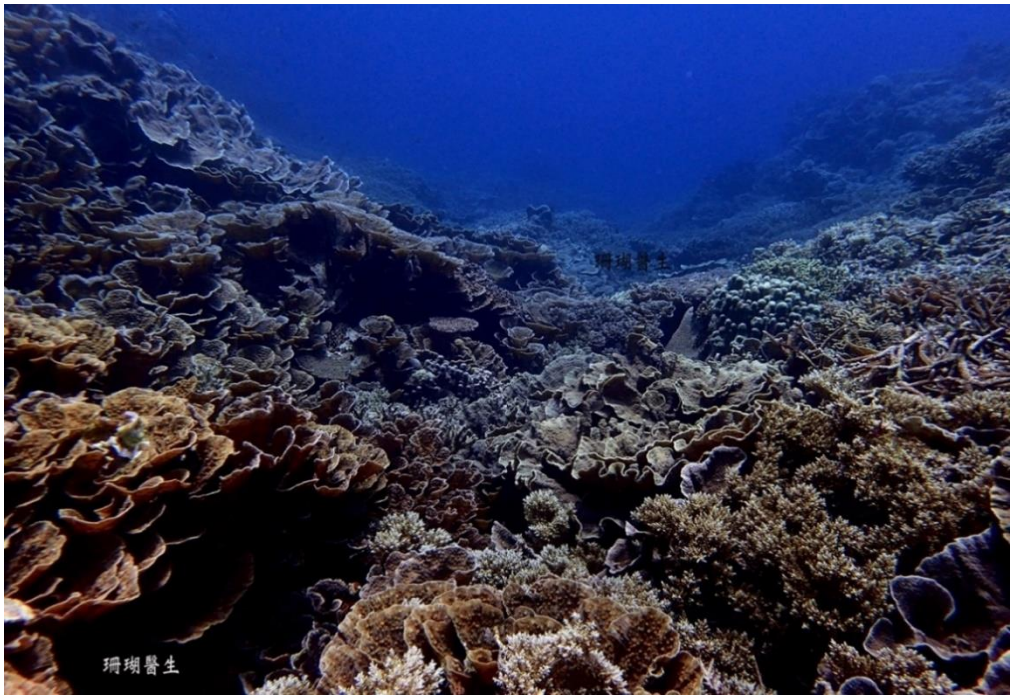

Fig. 1. A recently consolidated lava flow covered with scleractinian corals. "Lava Flow" dive site off Bandaneira, Maluku, Indonesia. Photo credit=Anderson Mayfield (a.k.a. 珊瑚醫生).

namely lipid trafficking, undergo a greater degree of regulation in response to changes in temperature (Mayfield, 2020; Mayfield et al., 2016b, 2018a). Barshis et al. (2013) interpreted this finding to reflect a desirable trait: the CSR is engaged perpetually to effectively thwart future, predictable shifts in the abiotic milieu. This indeed occurs in corals exposed to variable temperatures (Mayfield et al., 2011, 2012a), though why corals in relatively stable seawater temperature habits (1-2°C change/day) would adopt this strategy is puzzling, especially considering the high energy costs associated with maintaining the CSR (Hochachka & Somero, 2002). Canonical CSR should be ephemeral, though perhaps an "alternative stable state" may be reached in which, while still technically fit (growing & reproducing), coral-dinoflagellate cell biology may undergo profound alterations as a result of prior (or present) exposure to aberrant oceanographic conditions.

Thankfully, there is a wealth of knowledge on the environmental physiology of pocilloporid corals, particularly in Southern Taiwan (e.g., Mayfield et al., 2010, 2012b, 2013a,c, 2014a-b, 2016b-c, 2018a; Putnam et al., 2013; Mayfield, 2016; McRae et al., in

review), and a plethora of cellular and molecular tools for probing the cellular physiology of marine organism- (e.g., anthozoans, forams, & giant clams)-dinoflagellate (family Symbiodiniaceae) endosymbioses is currently at our disposal (e.g., Peng et al., 2011; Chen et al., 2012, 2015, 2017; Doo et al., 2012, 2014; Wang et al., 2013; Mayfield et al., 2014c; Lin et al., 2015, 2019; Monteiro et al., 2020). We sought herein to use the transcriptomic dataset from the "*Pocillopora acuta* long-term temperature experiment" (PALTTE; Mayfield et al., 2014d) to explore the idea of high-temperature-mediated alternative stable states by employing a number of both univariate and multivariate approaches *not* featured in the initial analysis. We specifically hypothesized that we could develop a molecular biology-trained model (*sensu* Mayfield & Chen, 2019) that could be used predict the degree to which coral biology has shifted as a result of GCC-induced stress.

Materials & Methods

The PALTTE. The experiment (formerly the "PDLTTE" since *P. damicornis* & *P. acuta* were synonymized at the time of analysis [2010-2011]; see Schmidt-Roach et al., 2014 & Mayfield et al., 2015.) was originally described by Mayfield et al. (2013b). Briefly, replicate colonies from Houbihu (Nanwan Bay, Taiwan) were fragmented into nubbins, suspended on fishing lines, and acclimated in flow-through seawater mesocosms (n=6) for several weeks prior to initiating a long-term high-temperature exposure of 29.7°C (rounded to 30°C hereafter). Control mesocosms (n=3) were instead maintained at 27°C. These customized, mesocosm-like aquarium systems have recently been found to result in the highest pocilloporid coral growth rates ever documented (Huang et al., 2020). Corals were sampled prior to the start of the temperature ramping, as well as after 2, 4, 8, 24, and 36 weeks. A subset of three nubbins from each of the two treatments was sacrificed after 2 and 36 weeks to assess the effect of relatively short- and long-term high-temperature exposure on gene expression (n=12 samples analyzed by RNA-Seq [Illumina Tru-Seq™ technology]). The gene expression findings were described in Mayfield et al. (2014d), with a subset of samples also analyzed by two-dimensional gel electrophoresis followed by mass spectrometry-based proteomics (Mayfield et al., 2018b). Although it was found that there was no congruency between the mRNA- and protein-level responses (as was the case in other corals [Mayfield et al., 2016c, in review; Mayfield, 2020]), we nevertheless hypothesized that the gene expression data could be useful in identifying biomarkers (univariate

approach) and/or developing models (multivariate approach) that would enable us to understand whether to-be-sampled conspecifics *in situ* are exhibiting cellular hallmarks of chronic high-temperature exposure (i.e., the aforementioned alternative stable states).

Meta-analysis of the* P. acuta-Cladocopium *spp. transcriptome. The holobiont (host coral+dinoflagellates+ bacteria & other microbes) transcriptome of Mayfield et al. (2014d) was downloaded from our interactive transcriptome server (http://symbiont.iis.sinica.edu.tw/coral_pdltte/static/html/index.html#home), and the fragments per kilobases mapped (FPKM) data were re-analyzed using a series of both univariate and multivariate statistical approaches (MSA). Please note that, although the transcriptome features 236,435 genes, certain analyses incorporated subsets of this total. A diagnostic analysis was first undertaken in which normal quantile box plots of log_2-transformed expression levels (n=202,283 genes only since bacterial, viral, & non-expressed genes were excluded.) were produced to depict general temperature x time trends for each compartment (coral host vs. dinoflagellates); the specific goals of this analysis were to determine whether 1) the hosts or their endosymbionts demonstrate higher mean gene expression levels and 2) a relatively higher proportion of genes is differentially regulated in response to temperature stress in one compartment vs. the other.

MSA. Principal components analysis (PCA) on correlations and multi-dimensional scaling (MDS) were carried out with JMP® Pro (ver. 15, USA) with raw and standardized FPKM data, respectively; JMP Pro was used for all remaining analyses unless noted otherwise. Because the "robust PCA" method uncovered an outlier (C36T2S1), the approaches outlined below generally excluded this sample. This resulted in an unbalanced design in which there were three, three, two, and three control-2-week (C2), high-temp.-2-week (H2), control-36-week (C36), and high-temp.-36-week (H36) samples, respectively. A Venn diagram was used to depict overlap in the transcriptomes of these samples, and permutational multivariate ANOVA (PERMANOVA; PRIMER, ver. 6, UK) was used to assess the effects of temperature (control vs. high), time (2 vs. 36 weeks), and their interaction on the similarity among the 11 samples (Euclidean distance matrix using standardized data). An unrestricted permutation of raw data (sum of squares, type III) model was employed (alpha=0.05). A repeated measures design was not adopted since independent nubbins were sacrificed within each

mesocosm at each sampling time. PERMDISP was conducted to ensure that multivariate dispersion did not differ significantly across treatments. Because PRIMER can only analyze <65,000 data points, simple random samples (SRS) of ~65,000 genes were taken from the transcriptome, and analyses were run 3-4 times.

Transcriptomic predictive modeling. In addition to uncovering 1) multivariate treatment effects on the *P. acuta*-*Cladocopium* spp. dinoflagellate transcriptome (above) and 2) differentially expressed genes (DEGs; below), there was an interest in developing models that could be used to predict the susceptibility of a coral sample to high temperatures based on its gene expression profiles. In this particular experiment, in which all corals ultimately acclimated to temperatures approaching 30°C, this endeavor additionally sought to characterize the "acclimatome" of this model coral species. If we can characterize the diagnostic features of a coral that has effectively acclimated to high temperatures in the laboratory, then perhaps we could sample a coral from the field in which we know nothing about its physiology, input the data into the experimental model derived herein, and make predictions as to its acclimatization potential (or determine whether it has entered an alternative stable state). Ideally, stressed samples would be included in such an analysis, but, based on our physiological (Mayfield et al., 2013b) and molecular (Mayfield et al., 2014d) data, these coral nubbins appeared to have acclimated to 30°C. JMP Pro 16 beta's "model screening" algorithm was used with temperature (control vs. high) as the Y and the 236,435 genes as predictors (X). Seven different models capable of accommodating categorical response variables (binomial in this case: control vs. high) were built in tandem (n=4 unique iterations), with seven and four training and validation (i.e., hold-back) samples, respectively. These models included nominal logistic, support vector machines, bootstrap forest, neural (boosted), generalized regression, K nearest neighbors, and naïve Bayes. The resulting validation model with the lowest 1) misclassification rate and 2) root mean square error (RMSE) was chosen as having the highest power to predict *in situ* coral temperature effects in future "test" samples (i.e., those *not* used in the model-building exercise and for which we know nothing). The mean misclassification rates and RMSE across the four iterations of the superior model were calculated and are the main model parameters discussed herein.

DEGs. A univariate approach was taken to uncover genes differentially expressed across temperatures, times, and

their interaction. Rather than use a more traditional false discovery rate (FDR)-based "response screen" exclusively, we instead first identified *only* those genes expressed by all samples in one treatment and in no samples of the opposing treatment. For instance, if a gene was expressed by all six control samples (including the outlier), and in none of the six high-temperature samples, it was considered a DEG. Response screening and predictor screening analyses were then used to corroborate these presence/absence DEGs. Of the 108 genes only expressed by H2 samples (online supplemental data file [OSDF]), real-time PCR (qPCR) assays were designed for a subset of 10: 9 from the dinoflagellates and 1 from the coral host (Tab. 1). Unlike for the MSA, all 12 mRNA samples were analyzed by qPCR after reverse transcription of 200 ng of RNA to cDNA using the High Capacity™ cDNA synthesis kit from Applied Biosystems (USA; 20 µL reactions using random primers following the manufacturer's recommendations). It should be noted that the same mRNA aliquots were used for RNA-Seq (Mayfield et al., 2014d) and qPCR. Reactions (20 µL) comprised 10 µL of 2X EZ-Time™ SYBR® Green I premix with ROX® passive reference dye (Yeastern, Taiwan), 2 µL of 4-fold diluted cDNA, and variable quantities of the forward and reverse primers (Tab. 1), which were synthesized (salt-free) by Eurofins Scientific (USA; 10-µM scale).

qPCRs were carried out in triplicate for each sample and gene on an Applied Biosystems 7500 real-time PCR machine as described in Tab. 1, using SYBR Green I and ROX as the target and reference dyes, respectively. Serial dilutions (1/1, 1/10, & 1/100-fold of a control sample made by mixing cDNA from a multitude of adult pocilloporid corals [200 ng mRNA equivalent in total]), as well as no-template controls, were run in triplicate on each 96-well plate before analyzing the experimental samples to optimize primer efficiency (sensu Mayfield et al., 2013d, 2014a). All assays described in Tab. 1 were characterized by 1) single peaks in the post-run melting curve analysis (65-95°C) and 2) PCR efficiencies between 90 and 110% (data not shown). Since endosymbiont densities did not vary dramatically across samples (Mayfield et al., 2013b), nor did the host/endosymbiont contig ratio differ significantly across the temperature x time interaction groups (Mayfield et al., 2014d & Fig. 2), the biological composition normalization featured in our prior analyses (e.g., Mayfield et al., 2009) was not undertaken; instead, the inverse of the qPCR threshold cycle (Ct) values was

Tab. 1. Real-time PCR (qPCR) assays for select genes found by RNA-Seq to be expressed only by high-temperature samples at the 2-week sampling time (H2). All genes with the exception of the tetratricopeptide repeat protein 28-like protein with a CHAT ("caspase HetF associated with Tprs") domain (hereafter "CHAT domain;" **Fig. 6**) were targeted in the Symbiodiniaceae ("Sym") endosymbionts exclusively. No Illumina-derived trends (i.e., expressed by H2 only) were supported entirely; at least some detectable level of expression was documented in 2-week control samples (C2) by qPCR. Instead, the qPCR-derived "H2>C2 fold change" values have been shown except for when they were not statistically significant (NS), and those for which the Illumina vs. qPCR R^2 (**Fig. 5**) values were statistically significant ($p<0.01$) have been denoted by asterisks (*). Genes involved the cellular stress response have been emphasized in **bold** font. Please note that the "PD" in the host primer names corresponds to *Pocillopora damicornis*, as *P. acuta* and *P. damicornis* were synonymized at the time of study. Bp=base pairs. TNF=tumor necrosis factor.

Primer name	Gene name/ Fig.	H2>C2 fold change	Transcriptome accession	Amplicon size (bp)	Sequence ('5-3')	[primer] nM	Annealing temp. (ºC)	Cycle #
Sym-20944-F1	unknown	16*	comp20944_c0_seq1	108	AGG-ACA-CCC-TGC-CGA-AAG-A	250	61	40
Sym-20944-R1	5A				CCA-GCA-CAC-CAA-ACG-CAC-AA			
Sym-cildyn6-F1	ciliary dynein 6	90*	comp22007_c0_seq1	59	GTA-TGA-GTT-TGA-GAT-TGT-GCC-GT	400	60	40
Sym-cildyn6-R1	5B				AGA-TGG-TCA-TGT-AAT-CGT-TGG-G			
Sym-DNAJ-F1	**DNAJ**	27	comp69860_c1_seq1	124	CTC-AGT-TCC-TCC-AGC-GCA-T	250	61	40
Sym-DNAJ-R1	5C				CAG-ACG-GTC-TTT-TTG-GTG-CCA-T			
Sym-E3-ubiq-lig-F1	**E3 ubiquitin ligase**	30*	comp76579_c2_seq1	156	GCA-CAG-GTG-GCA-GAC-ATT	500	60	35
Sym-E3-ubiq-lig-R1	5D				GTC-AGA-GAC-AAA-GCC-CAC-A			
Sym-flik-F1	flagellar hook-length control protein	23	comp56753_c1_seq1	110	CTC-TCC-TTG-GCT-CCA-CTT-T	500	59	40
Sym-flik-R1	5E				AAG-GCA-TTT-CAA-CAC-TAC-AGG-TC			
Sym-largeATP-F1	large ATP-binding protein	NSa	comp768642_c0_seq1	141	ACG-TGG-TTT-TCG-GAA-GAT-GG	250	61	40
Sym-largeATP-R1	5F				GGA-ACA-AAT-CAA-GTC-GCG-GA			
Sym-lrrcp-F1	leucine-rich repeat-containing protein	6*	comp22663_c0_seq1	132	ACA-GCA-ACA-AGC-CCG-AAG	500	59	40
Sym-lrrcp-R1	5G				TCC-ACG-TCG-CCC-ATT-TC			
Sym-spatacsin-F1	spatacsin	70*	comp28643_c0_seq1	148	GAT-GTT-TGC-GCC-TGT-GTC-TTC	500	60	40
Sym-spatacsin-R1	5H				TCG-GCT-TCC-CTC-TAC-TCC-T			
Sym-TNFrecep-F1	TNF receptor	13*	comp30872_c0_seq1	51	CCG-GCA-CTT-GGA-TGG-ATA-GA	150	61	40
Sym-TNFrecep-R1	5I				CCT-GGG-CAT-TAT-GTG-GGA-C			
PD-CHAT-F1	CHAT domain	5	comp44179_c0_seq1	73	CAG-GGA-AGG-AAG-CAC-ACG-A	500	61	35
PD-CHAT-R1	6				TTA-CGC-GGC-ATT-GGA-GGA-C			

[a]Finding instead contradicted: C2>H2 (no statistically significant Illumina vs. qPCR correlation).

Platax 17: 1-26, 2020
doi: 10.29926/platax.202012_17.0002

calculated as: $(1/(E^{Ct}))*(10^9)$, where "E" is the PCR efficiency (e.g., 2=100%). These values were directly regressed against the respective Illumina-derived FPKM values, and the statistical significance of the correlations was assessed with linear regression *t*-tests (alpha=0.01). An H2/C2 relative fold difference was also calculated from the qPCR data to determine whether, in addition to the statistical significance of the correlation itself, the two mRNA quantification methods yielded congruent results. All in-text error terms represent standard error of the mean (SEM) unless stated otherwise.

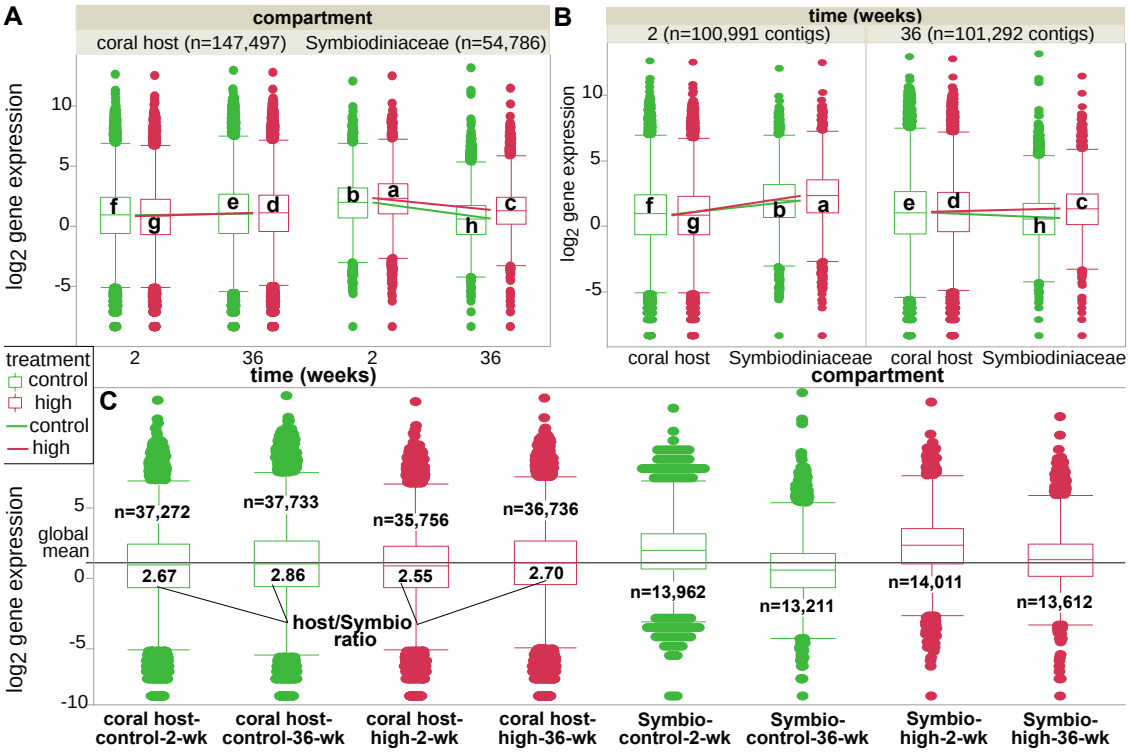

Fig. 2. PALTTE transcriptome diagnostic plots. Normal quantile box plots of log_2-transformed fragments per kilobases mapped values assessed across compartments (host coral vs. Symbiodiniaceae dinoflagellates) over time (A-C). Control (27ºC) and high-temperature (30ºC) samples have been colored green and red, respectively. In A and C, the sample sizes ("n=") reflect the number of sequenced contigs, whereas the lowercase letters within the box plots in A-B reflect Tukey's post-hoc inter-mean differences (p<0.05) across the eight temperature (df=1) x time (df=1) x compartment (df=1) interaction groups (Tab. 2). The values in the lower halves of the first four box plots (host coral) in C instead reflect the host coral/Symbiodiniaceae ("Symbio") contig ratios. In the x-axis label of C, "wk" corresponds to week, and the "global mean" log_2 gene expression level of ~1.1 has been plotted as a horizontal black line.

Tab. 2. Three-way ANOVA of the effects of temperature, time, and compartment on global coral holobiont gene expression. Fragments per kilobases mapped (FPKM) data from a subset of 227,615 contigs (FPKM>0; OSDF) were log_2-transformed prior to analysis, and the results of Tukey's post-hoc tests across all eight interaction groups (2 temperatures x 2 times x 2 compartments) can be seen in Fig. 2A-B. C2, H2, C36, and H36 correspond to the control and high-temperature samples at the 2- and 36-week sampling times, respectively. SS=sum of squares. Sym=Symbiodiniaceae dinoflagellates. Treatment=temperature treatment. ***p<0.001.

Source	SS	*F*	Multiple comparisons
compartment	14350	3048***	Sym>host
treatment	2898	615.5***	high>control
compartment x treatment	3032.1	644.0***	Sym-high(a)>Sym-control(b)>host-control(c)=host-high(c)
time	8969	1905.1***	2>36 weeks
compartment x time	18601	3951***	Sym-2(a)>host-36(b)>Sym-36(c)>host-2(d)
treatment x time	599.3	127.3***	H2(a)>C2(b)>H36(c)>C36(d)
compartment x treatment x time	125.5	26.66***	Fig. 2

Results & Discussion

Meta-analysis. Although there were approximately 3-fold more contigs of host coral (~150,000) than endosymbiont (~50,000) origin (Fig. 2A), the mean log_2-transformed FPKM level of 1.55±0.01 of the latter compartment was significantly higher than that of the former (0.94±0.01; Tab. 2). In fact, all effects in the 3-way ANOVA (Tab. 2) were statistically significant, and the compartment x treatment x time interaction effects have been depicted in Fig. 2. Within the host fraction, the mean log_2-transformed expression level did not differ between the 75,005 control and 72,492 high-temperature genes when pooled across times (though post-hoc interaction effects were nevertheless evident; Fig. 2A). In contrast, the mean 36-week expression level of 1.04±0.01 was significantly higher than that of the 2-week time (0.83±0.01; see post-hoc groups in Fig. 2A.). This signifies that sampling time more dramatically influenced coral gene expression levels than did temperature. Although the primary goal of this work was to assess temperature-mediated, rather than exclusively temporal, effects, the seasonal (2-week time=winter & 36-week time=summer) difference in global gene expression is interesting and possibly due to changes in the light environment: mean summer levels>mean winter levels on account of the mesocosms being exposed to ambient, albeit shaded, light (Mayfield et al., 2013b, 2014a). Indeed, others (e.g., Fitt et al., 2000) have documented seasonal changes in tissue biomass and the biochemical makeup of the holobiont,

which would likely be associated with changes in expression of numerous genes of both host and endosymbiont origin.

Global Symbiodiniaceae gene expression levels were instead higher at the 2-week sampling time (Fig. 2A-B & Tab. 2), and dinoflagellate gene expression was higher at high temperature at both sampling times (Fig. 2A-B), as well as when pooled across both (Tab. 2). Because there were no post-hoc differences between the host-high-temperature and host-control temperature groups in the 3-way ANOVA (Tab. 2), whereas such a temperature-related difference was documented for Symbiodiniaceae, we take this to signify that high-temperature exposure more significantly influenced the Symbiodiniaceae transcriptome than that of their coral hosts; this is the same conclusion made in our initial analysis of this dataset (Mayfield et al., 2014d), which was instead based on our having documented a relatively higher number of FDR-governed DEGs in the endosymbiont fraction vs. their hosts. The host/endosymbiont contig ratio (a proxy for the biomass ratio) was approximately 2.5-3:1 (Fig. 2C) and did not vary significantly in response to temperature. This is slightly lower than the mean ratio value of 3.3:1 reported by Mayfield et al. (2014d) for this same dataset and may be due to the fact that a larger percentage of Symbiodiniaceae contigs were successfully annotated herein given the recent growth in bioinformatics databases (Lin et al., 2015). In other words, *P. acuta* is approximately 2/3 animal, and 1/3 plant from an mRNA (& likely functional) perspective. However, in this analysis, the identity of the genes was not considered, only their concentrations. To gain insight into the thermo-biology of the holobiont, it is actually preferable to consider each individual gene in the analysis in a strictly multivariate framework so that transcriptomic similarity among samples or groups of samples may be discerned; this is the topic of the next section.

Multivariate effects. As for the global mean expression analysis of the host coral genes (Fig. 2 & Tab. 2), time more significantly affected the multivariate transcriptome than did temperature when using a more rigorous multivariate approach that considers the concentrations of each individual gene, PERMANOVA, with ~65,000-contig SRS of the data (Tab. 3). In no iteration was there a significant effect of temperature on the holobiont transcriptome, whereas there was always a highly significant temperature effect. This seasonal effect is not evident in the Venn diagram (Fig. 3A), in which ~45-50% of genes were

Tab. 3. Permutational multivariate ANOVA (PERMANOVA) of the effects of temperature, time, and their interaction on the *Pocillopora acuta-Cladocopium* spp. transcriptome. Data were standardized prior to creating the Euclidean distance matrix such that each protein was weighted evenly. Please note that, because the experimentally fragmented nubbins were independent from one another (& not repeatedly sampled), a 2-way PERMANOVA (rather than a repeated measures ANOVA) was performed. Since PRIMER (ver. 6) can only analyze ~65,000 analytes in a single analysis, simple random samples (SRS) of 65,000 contigs were taken thrice from the entire transcriptome. There were no statistically significant PERMDISP effects for temperature, time, or their interaction (p>0.05) in any of the three SRS.

Source of variation	df	Pseudo-*F*	#permutations	*p*
SRS-1 (n=63,364 contigs)				
Temperature (temp.)	1	1.320	991	0.103
Time	1	2.448	986	**0.001**
Temp. x time	1	0.976	985	0.423
Residual (SRS-1)	7			
SRS-2 (n=63,781 contigs)				
Temp.	1	1.329	988	0.099
Time	1	2.443	981	**0.001**
Temp. x time	1	0.977	981	0.403
Residual (SRS-2)	7			
SRS-3 (n=63,757 contigs)				
Temp.	1	1.319	985	0.076
Time	1	2.443	990	**0.001**
Temp. x time	1	0.973	987	0.415
Residual (SRS-3)	7			

expressed by samples of all four interaction groups. However, the multivariate time effect *can* be seen in the MDS plot (Fig. 3B). Although the ellipses do not signify clustering, there is nevertheless separation between the short- ("S;" 2-week) and long-term ("L;" 36-week) sampling times. In contrast, the control (green) and high-temperature samples (red) are only dissimilar after 36 weeks. However, since one C36 sample was excluded, this 36-week temperature difference cannot be interpreted with confidence. Furthermore, there was no interaction of temperature and time in the PERMANOVA (Tab. 3).

Predictive modeling. JMP Pro's model screening platform found that only the neural boosted algorithm, which is based on artificial intelligence, was able to develop a model for which the R^2 did not vary dramatically between the training and validation incarnations; this resulted in low misclassification rates and RMSE in

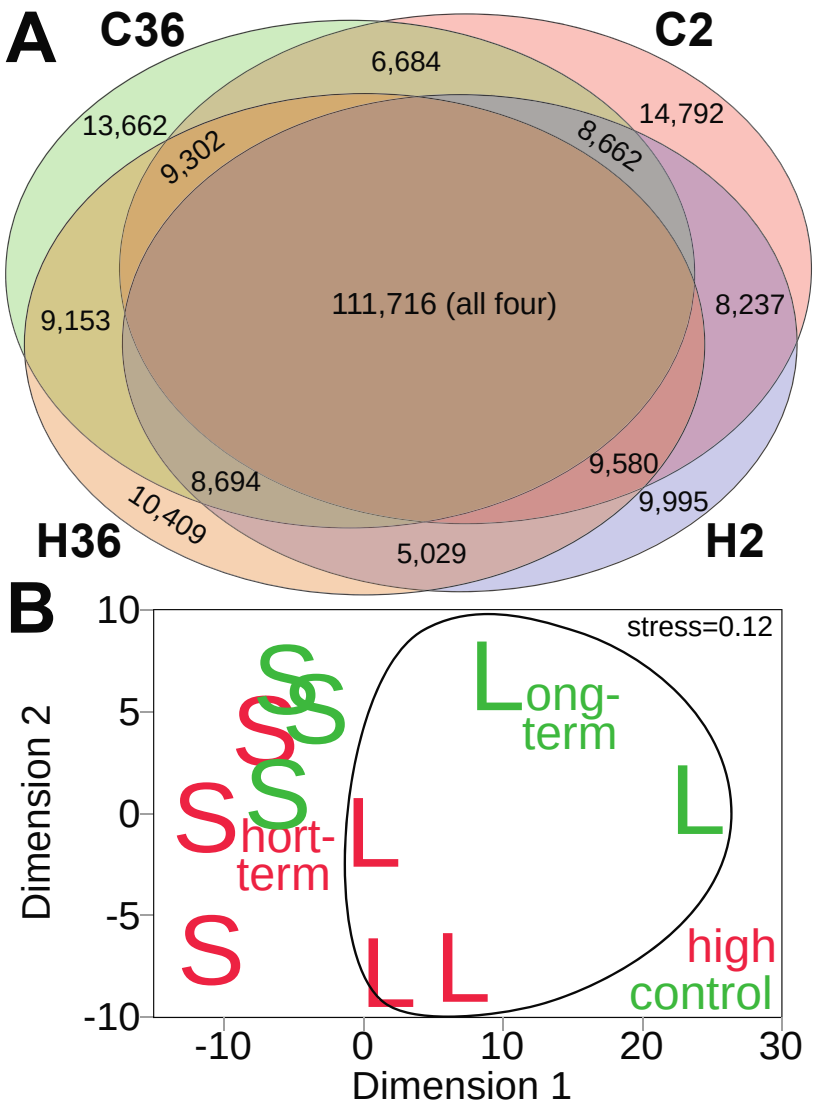

Fig. 3. Venn diagram (A) depicting overlap in expressed contigs across the control and high-temperature samples of the 2- and 36-week sampling times (C2, H2, C36, & H36, respectively) and a multi-dimensional scaling (MDS) plot (B) of 11 of the 12 transcriptome samples. Please note that several overlap groups are obscured in A and so the corresponding values do not sum to the contig total of 236,435. For MDS (B), one control sample at the 36-week sampling time (C36T2S1) was found to be a "robust PCA" (JMP® Pro) outlier and was excluded from analysis. Green and red icons represent control and high-temperatures samples, respectively, and the short (2-week) and long-term (36-week) sampling times are represented by "S" and "L," respectively. A principal coordinates ordination (not shown; PRIMER) found that the first and second dimensions captured 23.7 and 11.8% of the collective variation, respectively.

the four iterations (Fig. 4). The actual models are complex, though can be shared upon request. The fact that the neural boosted model could call 100% of the samples accurately with respect to treatment means that, were we to analyze a coral biopsy for which nothing is known with respect to its resilience, the gene expression data could be input into the model to make a guess as to whether that coral was healthy (i.e., predicted as being a control) or potentially in an alternative stable state with respect to chronic high-temperature exposure. Since the corals used in model training were presumably unstressed, this model cannot determine whether a coral is stress-susceptible or resilient; instead, if a coral is predicted to be a high-temperature sample by the model, this could actually signify that the coral has been acclimating to high temperatures for at least 2, or upwards of 36 weeks. In theory, the stress or acclimation/acclimatization response should be ephemeral (Cruz-Garcia et al., 2020); however, since the stressor was never eliminated at any point over the course of the study (e.g., no return to ambient temperatures at night), yet the expression levels of certain genes remained distinct between control and high-temperature samples at the final sampling time, this could signify that the corals had reached a physiological response plateau whereby, while not technically stressed, they were demonstrating an aberrant transcriptomic profile that may have underlaid their capacity to survive at 30ºC over such a prolonged duration. Similar results (albeit at the protein level) were obtained in Caribbean *Orbicella faveolata* specimens after a multi-week exposure to an ambient (presumably "control") temperature of 30ºC (Mayfield et al., in review).

DEGs. For the purposes of biomarker profiling, binary (presence/absence) data are preferable; this is because gene expression data are nearly always "noisy," highly variable, and skewed. If a thermal stress-associated gene, for instance, is expressed at 2-fold higher levels in corals exposed to high temperatures, and the expression levels of this gene are measured in test (i.e. field) samples, it will be difficult to discern based on expression of this gene alone whether the coral is undergoing cellular stress given said variability (not to mention the generally high concentrations of CSR genes/proteins discussed above). In contrast, if a gene is identified that is *only* expressed at high temperatures, and never in control samples (or vice versa), this would represent a superior biomarker. For that reason, we used conditional arguments to identify those genes in the transcriptome that were 1) only in the H2 treatment (& not in the 2-

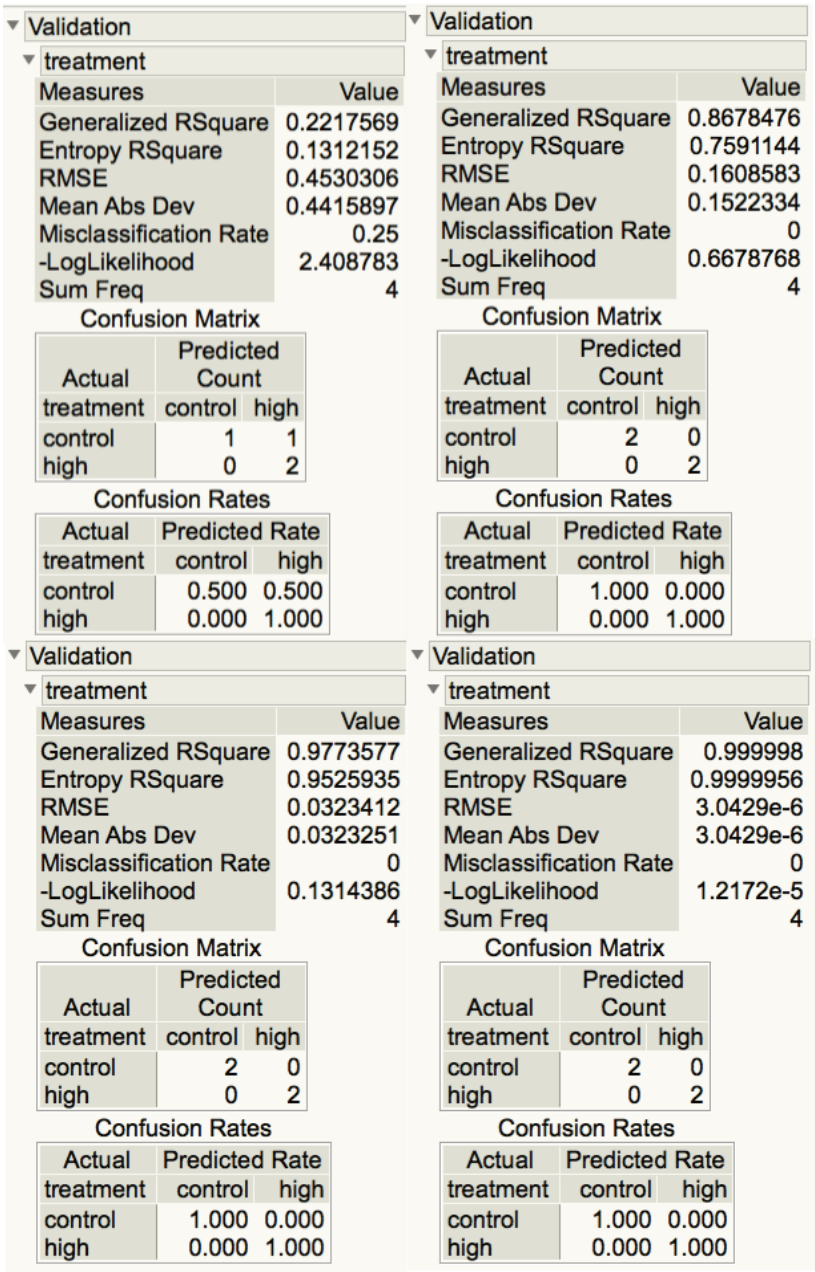

Validation

treatment

Measures	Value
Generalized RSquare	0.2217569
Entropy RSquare	0.1312152
RMSE	0.4530306
Mean Abs Dev	0.4415897
Misclassification Rate	0.25
-LogLikelihood	2.408783
Sum Freq	4

Confusion Matrix

Actual	Predicted Count	
treatment	control	high
control	1	1
high	0	2

Confusion Rates

Actual	Predicted Rate	
treatment	control	high
control	0.500	0.500
high	0.000	1.000

Validation

treatment

Measures	Value
Generalized RSquare	0.8678476
Entropy RSquare	0.7591144
RMSE	0.1608583
Mean Abs Dev	0.1522334
Misclassification Rate	0
-LogLikelihood	0.6678768
Sum Freq	4

Confusion Matrix

Actual	Predicted Count	
treatment	control	high
control	2	0
high	0	2

Confusion Rates

Actual	Predicted Rate	
treatment	control	high
control	1.000	0.000
high	0.000	1.000

Validation

treatment

Measures	Value
Generalized RSquare	0.9773577
Entropy RSquare	0.9525935
RMSE	0.0323412
Mean Abs Dev	0.0323251
Misclassification Rate	0
-LogLikelihood	0.1314386
Sum Freq	4

Confusion Matrix

Actual	Predicted Count	
treatment	control	high
control	2	0
high	0	2

Confusion Rates

Actual	Predicted Rate	
treatment	control	high
control	1.000	0.000
high	0.000	1.000

Validation

treatment

Measures	Value
Generalized RSquare	0.999998
Entropy RSquare	0.9999956
RMSE	3.0429e-6
Mean Abs Dev	3.0429e-6
Misclassification Rate	0
-LogLikelihood	1.2172e-5
Sum Freq	4

Confusion Matrix

Actual	Predicted Count	
treatment	control	high
control	2	0
high	0	2

Confusion Rates

Actual	Predicted Rate	
treatment	control	high
control	1.000	0.000
high	0.000	1.000

Fig. 4. Results of four iterations of a boosted neural networking model capable of predicting coral temperature dosing (control vs. high). In this simulation, four samples were randomly left out for validation with the other seven used for training (the outlier mentioned above was not considered.). Three of the four models were characterized by 0% misclassification rates in the validation stage (mean=6% of samples misclassified with respect to temperature across all four iterations), and the mean root mean square error (RMSE) was 0.16±0.10 (SEM).

week controls; n=108; OSDF), 2) only in the H36 treatment (& in none of the 36-week controls; n=105; OSDF), 3) only in the six high-temperature samples (& in none of the six control samples; n=10; Tab. 4), and 4) only in the six control-temperature samples (& in none of the six high-temperature samples; n=12; Tab. 4). Of these 213 new presence/absence DEGs, a SRS of 40 H2-only and 53 H36-only DEGs were annotated, and 17 (43%) and 40 (75%), respectively, failed to align to any published sequence on the NCBI database. Of the 40 H2-only DEGs (**OSDF**), 18 (45%) were of Symbiodiniaceae origin; this represents a marginally statistically significant over-representation versus the overall holobiont composition of ~70/30 host/endosymbiont (X^2 test, p=0.05). In contrast, only 3 of the 53 annotated DEGs of the 36-week sampling time were of endosymbiont origin (6%). Although it is tempting to take the 18 endosymbiont vs. 9 host coral annotated DEGs (i.e., 1:2 host:endosymbiont ratio) to signify that the endosymbiont compartment is more thermo-sensitive (as discussed above using alternative approaches), it is possible that the vast majority of the unknown contigs might be of host coral origin, in which case the DEG breakdown might actually not differ significantly from the 2:1 host:endosymbiont ratio of Mayfield et al. (2014d).

For a subset of DEGs expressed only by H2, qPCR assays were developed (Tab. 1), and the presence/absence data were *not* corroborated (Figs. 5-6); at least some level of expression (Ct<35) was documented for each of the nine endosymbiont (Fig. 5A-I) and one coral (Fig. 6) gene. That said, the H2>C2 effect was verified for all genes except for the large ATP-binding protein (Fig. 5F). Furthermore, given the generally large fold differences over controls (~25; Tab. 1), it is still possible that these DEGs might be used as biomarkers for assessing sub-lethal thermal stress, or a shift to an alternative stable state, for those without sufficient funds for RNA-Seq (~$150/sample as of September 2020). If we can ultimately rank corals along a spectrum (Fig. 7), from highly bleaching-prone to markedly GCC-resistant (i.e., successfully acclimatizing &/or adapting), the resulting triage capacity will allow us inform managers as to which reefs may be beyond saving, as well as which may instead be refugia (e.g., Cacciapaglia & van Woesik, 2016; Tortolero-Langarica et al., 2016; Rodriguez-Troncoso et al., 2019).

Acknowledgements

Thanks are given to those who made charitable contributions to the

Tab. 4. Differentially expressed genes (DEGs). Please note that the multivariate outlier, C36T2S1, was maintained in this analysis. Samples in **bold** and denoted by asterisks (*) were identified by response screening (FDRlogworth≥1) and predictor screening (>2% of the variation due to temperature, time, or their interaction explained), respectively. Of the 22 DEGs, 9, 4, 1, and 8 were of host coral (41%), endosymbiont (18%), bacterial (5%), and unknown (36%) origin, respectively. The functions of only 8 (36%) could be inferred via homology searches against public databases (e.g., NCBI, KEGG, pFAM), and 3 such DEGs (14%) were involved in nucleotide metabolism. The second most common cellular process identified was receptor (2/22=9%). Temp.=temperature.

accession	identity	function	compartment	genome accession
High temp.-only: all 6 high-temp. samples & 0 of the 6 control samples (n=10)				
comp80172_c0_seq2*	GMP synthase glutamine-hydrolyzing	nucleotide metabolism	endosymbiont	OLP90795.1
comp82751_c0_seq1*	unknown	unknown	unknown	no hit
comp86677_c0_seq1	unknown	unknown	unknown	no hit
comp111636_c0_seq10	unknown with CUB domain	unknown	coral host	XP_027057486
comp112485_c0_seq4	serine/threonine-protein phosphatase 6 regulatory ankyrin repeat subunit C-like	signaling	coral host	XP_027060124.1
comp114802_c0_seq3	unknown	unknown	coral host	XP_027057972
comp123755_c0_seq19	oncoprotein-induced transcript 3 protein-like	unknown	coral host	XP_027043126
comp265791_c0_seq1	unknown	unknown	unknown	no hit
comp331820_c0_seq1	unknown	unknown	unknown	no hit
comp390759_c0_seq1	unknown	unknown	weak bacterial hit	
Control temp.-only: all 6 control samples & 0 of the 6 high-temp. samples (n=12)				
comp49375_c0_seq1	glucosyltransferase[a]	protein modification	coral host	XP_027056940
comp55964_c0_seq1	unknown	unknown	endosymbiont	weak hit
comp62421_c1_seq1	protein GRPE	transport	endosymbiont	OLQ04308
comp64413_c1_seq1	unknown	unknown	unknown	no hit
comp98703_c0_seq1	unknown	unknown	unknown	no hit
comp115002_c0_seq2	3'5'-cyclic nucleotide phosphodiesterase	nucleotide metabolism	coral host	XP_027050742
comp115250_c3_seq2	sphingosine 1-phosphate receptor 3-like	receptor	coral host	XP_027043046
comp120597_c2_seq1	unknown	unknown	unknown	no hit
comp120797_c2_seq11	neuropeptide Y receptor type 1-like	receptor	coral host	XP_027051642.1
comp121122_c1_seq29	cAMP & cAMP-inhibited cGMP 3',5'-cyclic phosphodiesterase 10A	nucleotide metabolism	coral host	XP_027040302
comp123092_c0_seq22	unknown	unknown	endosymbiont	weak hit
comp661593_c0_seq1	unknown	unknown	unknown	no hit

[a]full name: probable dolichyl pyrophosphate Glc1Man9GlcNAc2 alpha-1,3-glucosyltransferase isoform X3.

Platax 17: 1-26, 2020
doi: 10.29926/platax.202012_17.0002

Friendly Bear Editorial service (http://coralreefdiagnostics.com/fbes), as well as the MacArthur Foundation for funding the laboratory analyses. The views expressed herein are the authors' own and do not necessarily reflect those of the United States government.

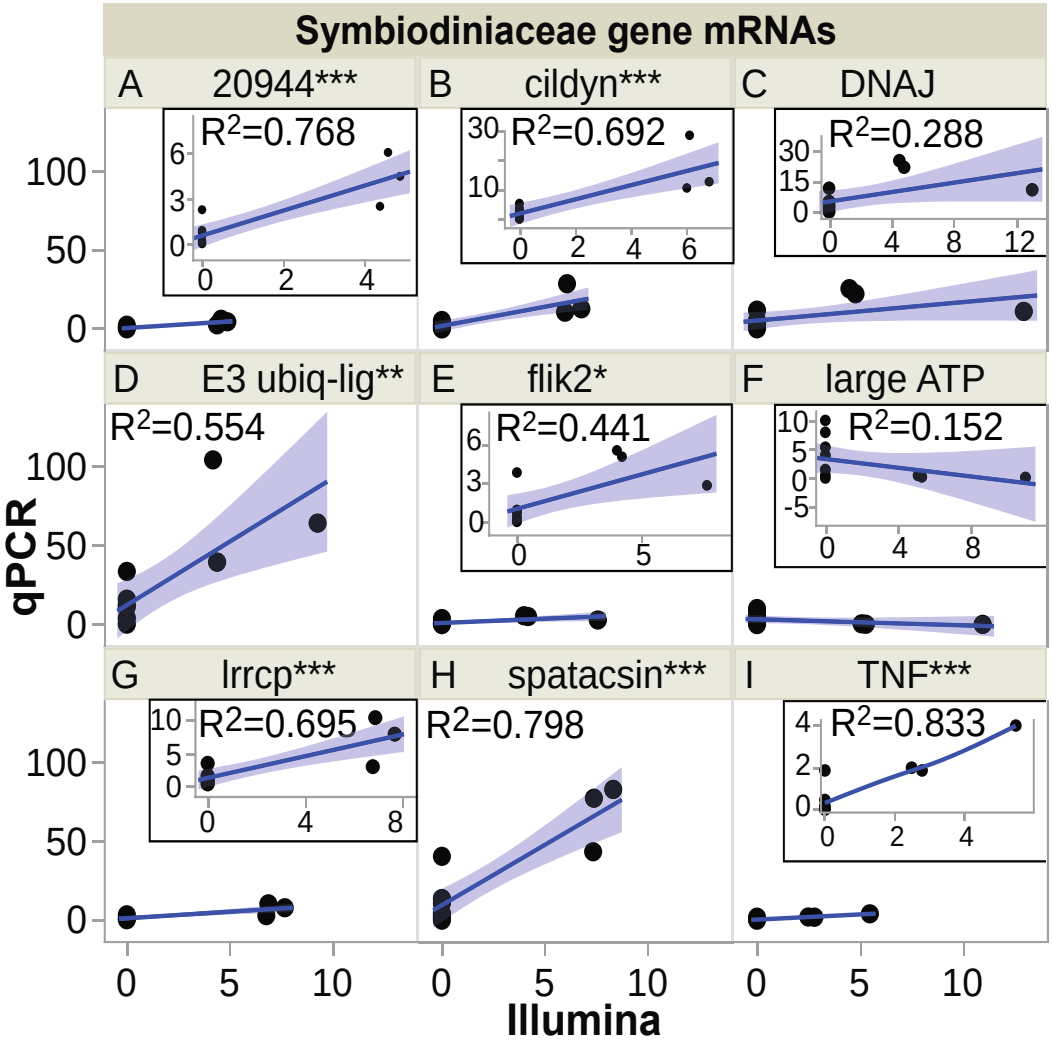

Fig. 5. Correlations between RNA-Seq (Illumina) and qPCR data for nine Symbiodiniaceae genes found by the former approach to be only expressed by high-temperature samples sacrificed after two weeks. Since all qPCR data (y-axes) were plotted on the same scale, insets have been placed within all but two panels to better demonstrate the linear relationships. Statistically significant linear correlations have been denoted by *(p<0.05), **(p<0.01), or ***(p<0.001). The blue bands about the trend lines represent 95% confidence.

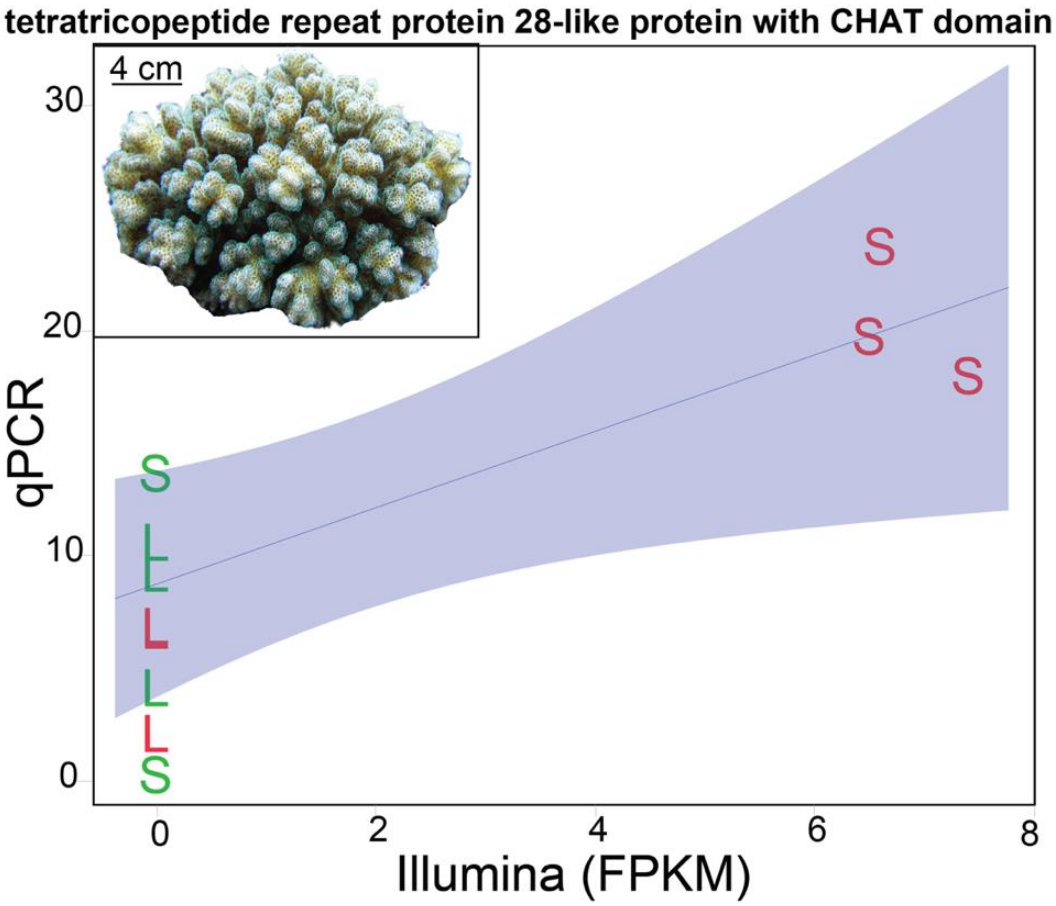

Fig. 6. Correlation between qPCR and RNA-Seq (Illumina) data for a host coral gene found by the latter approach to only be expressed by high-temperature samples at the 2-week sampling time: tetratricopeptide repeat protein 28-like protein with CHAT domain. An inset of an experimental coral from which "nubbins" were made for the PALTTE has been displayed in an inset. FPKM=fragments per kilobases mapped.

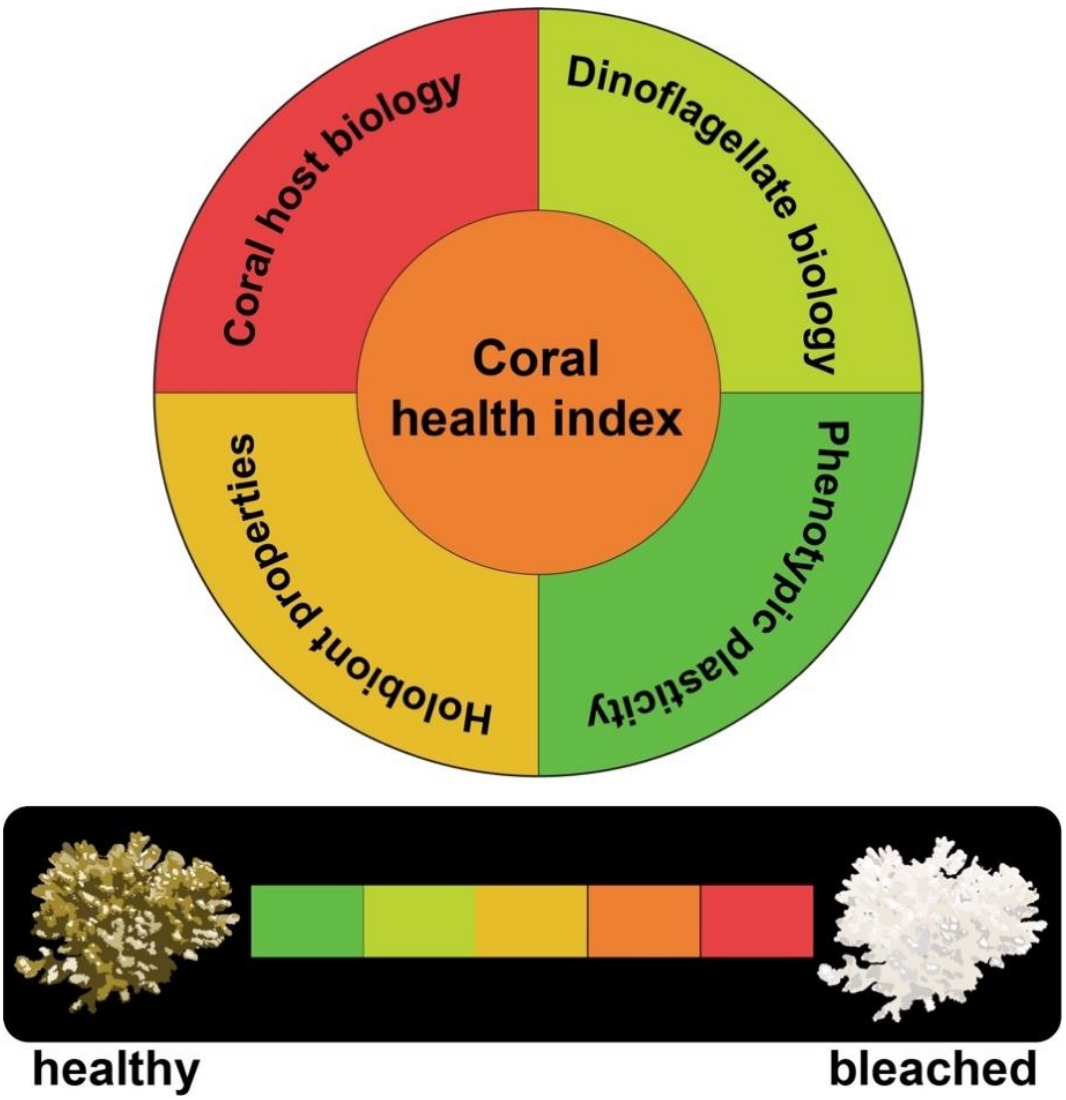

Fig. 7. A hypothetical coral health index. This index incorporates response variables from the anthozoan host alone ("Coral host biology"), the dinoflagellate compartment alone ("Dinoflagellate biology"), and the holobiont as a composite unit ("Holobiont properties"). The latter includes not only microbes (e.g., bacteria & viruses) but also larger invertebrates that associate with corals, like copepods (Cheng et al., 2016). A fourth wedge, "Phenotypic plasticity" reflects both spatio-temporal and environmental variation in physiological performance, as well as deviance from the mean phenotype established for the species in question (i.e., degree of aberrant behavior).

References

Barshis D.J., J.T. Ladner, T.A. Oliver, F.O. Seneca, N. Traylor-Knowles & S.R. Palumbi. 2013. Genomic basis for coral resilience to climate change. Proceedings of the National Academy of Sciences of the United States of America, 110:1387-1392.

Brown, B.E. 1997. Coral bleaching: causes and consequences. Coral Reefs, 16:s129-s138.

Brown, B.E., R.P. Dunne, M.S. Goodson & A.E. Douglas. 2000. Bleaching patterns in reef corals. Nature, 404:142.

Cacciapaglia, C. & R. van Woesik. 2016. Climate-change refugia: shading reef corals by turbidity. Global Change Biology, 22:1145-1154.

Chen, H.K., A.B. Mayfield, L.H. Wang & C.S. Chen. 2017. Coral lipid bodies as the relay center interconnecting diel-dependent lipidomic changes in different cellular compartments. Scientific Reports, 7:3244.

Chen, H.K., S.N. Song, L.H. Wang, A.B. Mayfield, Y.J. Chen, W.N.U. Chen, et al. 2015. A compartmental comparison of major lipid species in a coral-*Symbiodinium* endosymbiosis: evidence that the coral host regulates lipogenesis of its cytosolic lipid bodies. PLoS ONE, e0132519.

Chen, T.Y., G.W. Hwang, A.B. Mayfield, C.P. Chen & H.J. Lin. 2017. The relationship between intertidal soil composition and fiddler crab burrow depth. Environmental Engineering, 100:256-260.

Chen, T.Y., G.W. Hwang, H.J. Lin, A.B. Mayfield & C.P. Chen. 2019. The development of a habitat suitability model for sub-tropical tidal flat fiddler crabs. Ocean and Coastal Management, 182:104931.

Chen, W.N.U., H.J. Kang, V.M. Weis, A.B. Mayfield, L.S. Fang & C.S. Chen. 2012. Diel rhythmicity of lipid body formation in a coral-*Symbiodinium* endosymbiosis. Coral Reefs, 31:521-534.

Cheng, Y.R., P.J. Meng, A.B. Mayfield & C.F. Dai. 2016. Copepods associated with scleractinian corals: a worldwide checklist and a case study of their impact on the reef-building coral *Pocillopora damicornis* (Linnaeus, 1758) (Pocilloporidae). Zootaxa, 4174(1):291-345.

Chollett, I., P.J. Mumby & J. Cortés. 2010. Upwelling areas do not guarantee refuge for coral reefs in a warming ocean. Marine Ecology Progress Series, 416:47-56.

Cruz-García, R., A.P. Rodríguez-Troncoso, F.A. Rodríguez-Zaragoza, A.L. Cupul-Magaña & A.B. Mayfield. 2020. Ephemeral effects of El Niño southern oscillation events on an eastern tropical Pacific coral community. Marine and Freshwater Research, 71(10):1259-1268.

Doo, S.S., A.B. Mayfield, H.D. Nguyen & H.K. Chen. 2014. Protein analysis in large benthic foraminifera. Invited book chapter in: *Approaches to Study Living Foraminifera*. Editors: Hiroshi Kitazato and Joan Bernhard. Pp. 71-89.

Doo, S.S., A.B. Mayfield, M. Byrne, H.K. Chen, H. Nguyen & T.Y. Fan. 2012. Reduced expression of the rate-limiting carbon fixation enzyme RuBisCO in the benthic foraminifer *Baculogypsina sphaerulata* holobiont in response to heat shock. Journal of Experimental Marine Biology and Ecology, 430-431:63-67.

Enochs, I.C., N. Formel, D.P. Manzello, J. Morris, A.B. Mayfield, A. Boyd, et al. 2020. Coral persistence despite extreme periodic pH fluctuations at a volcanically acidified Caribbean reef. Coral Reefs, 39:523-528.

Fitt, W.K., F.K. McFarland, M.E. Warner & G.C. Chilcoat. 2000. Seasonal patterns of tissue biomass and densities of symbiotic dinoflagellates in reef corals and relation to coral

bleaching. Limnology & Oceanography, 45:677-685.

Gates, R.D. 1990. Seawater temperature and sublethal coral bleaching in Jamaica. Coral Reefs, 8:193-197.

Giovani, S. Escrig, A. Meibom, et al. 2017. Common reef-building coral in the Northern Red Sea resistant to elevated temperature and acidification. Royal Society Open Science, 4:170038.

Hochachka, P.W. & G.N. 2002. Biochemical adaptation. Oxford: Oxford University Press.

Hoegh-Guldberg, O., E.S. Poloczanska, W. Skirving & S. Dove. 2017. Coral reef ecosystems under climate change and ocean acidification. Frontiers in Marine Science, 4:158.

Huang, Y.C.A., H.J. Hsieh, S.C. Huang, P.J. Meng, Y.S. Chen, S. Keshavmurthy, et al. 2011. Nutrient enrichment caused by marine cage culture and its influence on subtropical coral communities in turbid waters. Marine Ecology Progress Series, 423:83-93.

Huang, Y.L., A.B. Mayfield & T.Y. Fan. 2020. Effects of feeding on the physiological performance of the stony coral *Pocillopora acuta*. Scientific Reports, 10:19988.

Krueger, T., N. Horwitz, J. Bodin, M.E. Giovani, S. Escrig, A. Meibom & M. Fine. 2017. Common reef-building coral in the Northern Red Sea resistant to elevated temperature and acidification. Royal Society Open Science, 4:170038.

Lee, H.J., S.Y. Chao, K.L. Fan, Y.H. Wang & N.K. Liang. 1997. Tidally induced upwelling in a semi-enclosed basin: Nan Wan Bay. Journal of Oceanography, 53:467-480.

Lin, C., S. Tsai & A.B. Mayfield. 2019. Physiological differences between cultured and wild coral eggs. Biopreservation and Biobanking, 17:370-371.

Lin, H.J., C.L. Lee, S.E. Peng, M.C. Hung, P.J. Liu & A.B. Mayfield. 2018. Anthropogenic nutrient enrichment may exacerbate the impacts of El Niño-Southern Oscillation (ENSO) events on intertidal seagrass beds. Global Change Biology, 24:4566-4580.

Lin, S., S. Cheng, B. Song, Z. Zhong, X. Lin, W. Li, et al. 2015. The *Symbiodinium kawagutii* genome illuminates dinoflagellate gene expression and coral symbiosis. Science, 350:691-694.

Liu, P.J., H.F. Chang, A.B. Mayfield & H.J. Lin. 2020. Influence of the seagrass *Thalassia hemprichii* on coral reef mesocosms exposed to ocean acidification and experimentally elevated temperatures. Science of the Total Environment, 700:134464.

Liu, P.J., K.N. Chung, L.L. Liu, W.H. Twan, J.T. Wang, M.Y. Leu, et al. 2012. Impacts of human activities on the coral reef ecosystems of southern Taiwan: a long-term study. Marine Pollution Bulletin, 64:1129-1135.

Liu, P.J., S.M. Lin, T.Y. Fan, P.J. Meng, K.T. Shao & H.J. Lin. 2009. Rates of overgrowth by macroalgae and attack by sea anemones are greater for live coral than dead coral under conditions of nutrient enrichment. Limnology and Oceanography, 54:1167-1175.

Mayfield A.B., A.W. Bruckner, C.H. Chen & C.S. Chen. 2015. A survey of pocilloporids and their endosymbiotic dinoflagellate communities in the Austral and Cook Islands of the South Pacific. Platax, 12:1-17.

Mayfield, A.B. & C.S. Chen. 2019. Enabling coral reef triage via molecular biotechnology and artificial intelligence. Platax, 16:23-47.

Mayfield, A.B. & R.D. Gates. 2007. Osmoregulation in anthozoan-dinoflagellate symbiosis. Comparative Biochemistry and Physiology-A: Molecular and Integrative Physiology, 147:1-10.

Mayfield, A.B. 2016. Uncovering spatio-temporal and treatment-derived

differences in the molecular physiology of a model coral-dinoflagellate mutualism with multivariate statistical approaches. Journal of Marine Science and Engineering, 4:63.

Mayfield, A.B. 2020. Proteomic signature of corals from thermodynamic reefs. Microorganisms, 8(8), 1171.

Mayfield, A.B. in review. Environmentally-mediated variation in New Caledonian reef corals. Atoll Research Bulletin.

Mayfield, A.B., A.C. Dempsey, C.S. Chen. in prep. Biomarker profiling in pocilloporid corals of the Solomon Islands.

Mayfield, A.B., A.C. Dempsey, J. Inamdar & C.S. Chen. 2018c. A statistical platform for assessing coral health in an era of changing global climate-I: a case study from Fiji's Lau Archipelago. Platax, 15:1-35.

Mayfield, A.B., C. Aguilar, I. Enochs & D.P. Manzello. in review. Shotgun proteomics of thermally challenged Caribbean reef corals. Coral Reefs.

Mayfield, A.B., C.S. Chen & A.C. Dempsey. 2017a. Biomarker profiling in corals of Tonga's Ha'apai and Vava'u archipelagos. PLoS ONE, e0185857.

Mayfield, A.B., C.S. Chen & A.C. Dempsey. 2017b. Identifying corals displaying aberrant behavior in Fiji's Lau Archipelago. PLoS ONE, e0177267.

Mayfield, A.B., C.S. Chen & A.C. Dempsey. 2017c. The molecular ecophysiology of closely related pocilloporid corals of New Caledonia. Platax, 14:1-45.

Mayfield, A.B., C.S. Chen & A.C. Dempsey. 2019a. Modeling environmentally-mediated variation in reef coral physiology. Journal of Sea Research, 145:44-54.

Mayfield, A.B., C.S. Chen & P.J. Liu. 2014a. Decreased green fluorescent protein-like chromoprotein gene expression in specimens of the reef-building coral *Pocillopora damicornis* undergoing high temperature-induced bleaching. Platax, 11:1-23.

Mayfield, A.B., C.S. Chen, A.C. Dempsey & A.W. Bruckner. 2016a. The molecular ecophysiology of closely related pocilloporids from the South Pacific: a case study from the Austral and Cook Islands. Platax, 13:1-25.

Mayfield, A.B., L.H. Wang, P.C. Tang, Y.Y. Hsiao, T.Y. Fan, C.L. Tsai, et al. 2011. Assessing the impacts of experimentally elevated temperature on the biological composition and molecular chaperone gene expression of a reef coral. PLoS ONE, e26529.

Mayfield, A.B., M. Chen, P.J. Meng, H.J. Lin, C.S. Chen & P.J. Liu. 2013a. The physiological response of the reef coral *Pocillopora damicornis* to elevated temperature: results from coral reef mesocosm experiments in Southern Taiwan. Marine Environmental Research, 86:1-11.

Mayfield, A.B., P.S. Chan, H.M. Putnam, C.S. Chen & T.Y. Fan. 2012a. The effects of a variable temperature regime on the physiology of the reef-building coral *Seriatopora hystrix*: results from a laboratory-based reciprocal transplant. The Journal of Experimental Biology, 215:4183-4195.

Mayfield, A.B., S. Tsai & C. Lin C. 2019b. The Coral Hospital. Biopreservation and Biobanking, 17:355-369.

Mayfield, A.B., T.Y. Fan & C.S Chen. 2013c. The physiological impact of *ex situ* transplantation on the Taiwanese reef-building coral *Seriatopora hystrix*. Journal of Marine Biology, Article ID 569369.

Mayfield, A.B., T.Y. Fan & C.S. Chen. 2013b. Physiological acclimation to elevated temperature in a reef-building coral from an upwelling environment. Coral Reefs, 32:909-921.

Mayfield, A.B., T.Y. Fan & C.S. Chen. 2013d. Real-time PCR-based gene expression analysis in the model reef-building coral *Pocillopora damicornis*: insight from a

salinity stress study. Platax, 10:1-29.

Mayfield, A.B., Y.B. Wang, C.S. Chen, S.H. Chen & C.Y. Lin. 2014d. Compartment-specific transcriptomics in a reef-building coral exposed to elevated temperatures. Molecular Ecology, 23:5816-5830.

Mayfield, A.B., Y.B. Wang, C.S. Chen, S.H. Chen & C.Y. Lin. 2016c. Dual-compartmental transcriptomic+proteomic analysis of a marine endosymbiosis exposed to environmental change. Molecular Ecology, 25:5944-5958.

Mayfield, A.B., Y.H. Chen, C.F. Dai & C.S. Chen. 2014b. The effects of temperature on gene expression in the Indo-Pacific reef-building coral *Seriatopora hystrix*: insight from aquarium studies in Southern Taiwan. International Journal of Marine Science, 4(50):1-23.

Mayfield, A.B., Y.J. Chen, C.Y. Lu & C.S Chen. 2016b. Proteins responsive to variable temperature exposure in the reef-building coral *Seriatopora hystrix*, in: Ortiz, S. (Ed.) Coral Reefs: Ecosystems, Environmental Impact and Current Threats. NOVA Publishing, New York, pp. 1-60.

Mayfield, A.B., Y.J. Chen, C.Y. Lu & C.S. Chen. 2018a. Exploring the environmental physiology of the Indo-Pacific reef coral *Seriatopora hystrix* using differential proteomics. The Open Journal of Marine Science, 8:223-252.

Mayfield, A.B., Y.J. Chen, C.Y. Lu & C.S. Chen. 2018b. The proteomic response of the reef coral *Pocillopora acuta* to experimentally elevated temperature. PLoS ONE, e0192001.

Mayfield, A.B., Y.Y. Hsiao, H.K. Chen & C.S. Chen. 2014c. Rubisco expression in the dinoflagellate *Symbiodinium* sp. is influenced by both photoperiod and endosymbiotic lifestyle. Marine Biotechnology, 16:371-384.

Mayfield, A.B., Y.Y. Hsiao, T.Y. Fan, C.S. Chen & R.D. Gates. 2010. Evaluating the temporal stability of stress-activated protein kinase and cytoskeleton gene expression in the Pacific corals *Pocillopora damicornis* and *Seriatopora hystrix*. Journal of Experimental Marine Biology and Ecology, 395:215-222.

Mayfield, A.B., Y.Y. Hsiao, T.Y. Fan, C.S. Chen. 2012b. Temporal variation in RNA/DNA and protein/DNA ratios in four anthozoan-dinoflagellate endosymbioses of the Indo-Pacific: implications for molecular diagnostics. Platax, 9:1-24.

McRae, C., A.B. Mayfield, T.Y. Fan TY & I. Cote. in review. Differing proteomic responses to high-temperature exposure between adult and larval reef corals. Marine Ecology Progress Series

Monteiro, H.J.A., C. Brahmi, B. Lapeyre, A.B. Mayfield & L. Le Luyer J. 2020. Molecular mechanisms of acclimation to long-term elevated temperature exposure in marine symbioses. Global Change Biology, 26:1271-1284.

Peng, S.E., W.N.U. Chen, H.K. Chen, C.Y. Lu, A.B. Mayfield, L.S. Fang, et al. 2011. Lipid bodies in coral-dinoflagellate endosymbiosis: ultrastructural and proteomic analyses. Proteomics, 17:3540-3455.

Putnam, H.M., A.B. Mayfield, T.Y. Fan, C.S. Chen & R.D. Gates. 2013. The physiological and molecular responses of larvae from the reef-building coral *Pocillopora damicornis* exposed to near-future increases in temperature and pCO_2. Marine Biology, 160:2157-2173.

Putnam, H.M., K. Barott, T.D. Ainsworth & R.D. Gates. 2017. The vulnerability and resilience of reef-building corals. Current Biology, 27:R528-R540.

Randall, C.J., L.T. Toth, J.J. Leichter, J.L. Maté & R.B. Aronson. 2020. Upwelling buffers climate change impacts on coral reefs of the eastern tropical Pacific. Ecology, 101(2):e02918.

Ribas-Deulofeu, L., V. Denis, S. De Palmas, C.Y. Kuo, H.J. Hsieh & C.A. Chen.

2016. Structure of benthic communities along the Taiwan latitudinal gradient. PLoS ONE, e0160601.

Rodríguez-Troncoso, A.P., F.A. Rodríguez-Zaragoza, A.B. Mayfield & A.L. Cupul-Magaña. 2019. Temporal variation in invertebrate recruitment on an Eastern Pacific coral reef. Journal of Sea Research, 145:8-15.

Safaie, A., N.J. Silbiger, T.R. McClanahan, G. Pawlak, D.J. Barshis, J.L. Hench, et al. 2018. High frequency temperature variability reduces the risk of coral bleaching. Nature Communications, 9:1-12.

Schmidt-Roach, S., K.J. Miller, P. Lundgren & N. Andreakis. 2014. With eyes wide open: a revision of species within and closely related to the *Pocillopora damicornis* species complex (Scleractinia; Pocilloporidae) using morphology and genetics. Zoological Journal of the Linnaean Society, 170:1-33.

Storlazzi, C.D., O.M. Cheriton, R. van Hooidonk, R. Z. Zhao, R. Brainerd. 2020. Internal tides can provide thermal refugia that will buffer some coral reefs from future global warming. Scientific Reports, 10:13435.

Tortolero-Langarica, J.J.A., A.L. Cupul-Magaña, J.P. Carricart-Ganivet, A.B. Mayfield & A.P. Rodriguez-Troncoso. 2016. Changes in growth and calcification rates in the reef-building coral *Porites lobata*: the implications of morphotype and gender on coral growth. Frontiers in Marine Science, 3(179).

UNEP. 2020. Projections of future coral bleaching conditions using IPCC CMIP6 models: climate policy implications, management applications, and Regional Seas summaries. United Nations Environment Programme, Nairobi, Kenya.

Wang, L.H., H.H. Lee, L.S. Fang, A.B. Mayfield & C.S. Chen. 2013. Normal fatty acid and phospholipid synthesis are prerequisites for the cell cycle of *Symbiodinium* and their endosymbiosis with sea anemones. PLoS ONE, e72486.